Desalination and Water Treatment
www.deswater.com
doi: 10.5004/dwt.2020.25724

190 (2020) 383–392
June

Phthalate-functionalized *Sorghum bicolor* L.; an effective biosorbent for the removal of Alizarin Red S and Bromophenol blue dyes from simulated wastewater

Momal Akram[a], Muhammad Salman[a,*], Umar Farooq[a], Umair Saleem[a], Samra Tahir[a], Huma Nazir[a,b], Hafiz Muhammad Arsalan[c]

[a]*Institute of Chemistry, University of the Punjab, Lahore-54590, Pakistan, emails: salman.chem@pu.edu.pk (M. Salman), momalakram96@gmail.com (M. Akram), umar.chem@pu.edu.pk (U. Farooq), umairsaleemchem@gmail.com (U. Saleem), stahir9523@gmail.com (S. Tahir), huma.nazir@ue.edu.pk (H. Nazir)*
[b]*University of the Education, Bank Road Campus, Lahore, Pakistan*
[c]*School of Biochemistry/Medical Lab Technology, Minhaj University Lahore, Pakistan, email: Arsalan.mlt@mul.edu.pk (H.M. Arsalan)*

Received 12 July 2019; Accepted 20 February 2020

ABSTRACT

This study aims to modify the agricultural waste, that is, *Sorghum bicolor* L. by means of phthalic anhydride for the enhanced removal of reactive dyes. This modified *Sorghum* was characterized by means of using Fourier-transform infrared spectroscopy-spectra, scanning electron microscope, pHpzc, and by Boehm's titration for the determination of acidic and basic groups. Alizarin Red S (ARS) and Bromophenol blue (BPB) were used as a substrate for removal. The observed optimum values were 0.1 g/50 ppm for ARS and 0.1 g/30 ppm for BPB at neutral pH within 25–30 min at room temperature. The equilibrium statistics fitted well in the Langmuir equilibrium model with maximum adsorption capacities of 285.71 and 65.78 mg g^{-1} for ARS and BPB, respectively. The kinetic data was followed by the pseudo-second-order rate equation. The thermodynamics study revealed that the process was exothermic and spontaneous.

Keywords: *Sorghum bicolor* L.; Alizarin Red S; Bromophenol blue; Non-linear isotherms; Kinetics; Thermodynamics

1. Introduction

Many industrial processes like in manufacturing of paper, rubber, food, plastics, cosmetics, leather, textile, paint, and the pharmaceuticals, large amount of synthetic dyes are utilized for the coloring of a variety of items and henceforward, their wastewater is also comprised of colors. In the dyeing process, about 50% of the dye is lost in wastewater because of the low level of fixation between dyes and surface to be dyed [1]. Globally, total dye consumption is more than 10,000 tons y^{-1} and from one valuation around 10%–20% colorants and annually 100 tons of dyes are discharged into water streams which are the main cause of dye polluted water [2,3]. The significant amount of dyes increases the upper limits of biochemical oxygen demand, chemical oxygen demand, total dissolved solids, and total suspended solids correspondingly [4].

Most of the dyes and their products are consisted of inorganic and mutagenic effect, causing harmful impacts to kidneys, reproductive system, respiratory system, and central nervous system can cause serious damage to both marine and human ecosystems because of their toxic properties which are a major threat to biota [5–10]. Because of complex synthetic structure, most of the dyes are resistant to heat and light and also makes them resistant to the aerobic and anaerobic digestions, stable to light, heat, and other biodegradation processes [11,12] so that's why as per

* Corresponding author.

of environmental viewpoint removal of synthetic dyes is of great apprehension. Thus, for these reasons wastewater consisting of dyes should be pre-treated before entering the environment.

The finest choice for dyes removal rest on the kinds, composition, and concentration of dyes presents in the wastewater. The physical, chemical, and biological strategies like coagulation, sedimentation, flocculation, membrane technology, ozonation, anaerobic and aerobic digestion, sonochemical degradation, electro-kinetic coagulation, electrochemical degradation, adsorption, ion exchange, biosorption, adsorption by activated carbon, and photochemical degradation was usually working designs for the elimination of dye [13,14]. Many of these processes have been known to be effective, but they have limitations also. Some of these techniques have been shown to be effective, although they have limitations. Among them are surplus use of chemicals, gathering of sludge and their disposal, the requirement of expensive instruments and sensitivity to different wastewaters [15]. Out of all the processes adsorption is of great interest because of its efficiency potential, low energy usage, high selectivity, a variety of chemical separation, and easy to operate.

The development of ecofriendly and new biosorbents for dyes removal is getting significant interest globally for researches [16]. Studies indicated that many constituents like chitosan, pine cone, kaolin, modified alumina, fly ash, raw mango seed, tea waste, cashew nutshells, orange peel, rice hull, modified sawdust, sugarcane bagasse, peanut husk, and activated bamboo waste were used as adsorbents which could effectively remove the dyes from wastewaters [7]. Biosorbent such as hazelnut shell [17], coconut coir dust [18], lotus leaf [19], *Carica papaya* wood [20], watermelon [21], *Haloxylon recurvum* [22], waste cotton seed [23], *Elaeagnus angustifolia* [24] were reported in the literatures for biosorption of dyes. This study is designed to develop a biosorbent grounded on *Sorghum bicolor* L. (SB) for dye removal through the reaction between the hydroxyl group of *Sorghum* and phthalic anhydride (PA). Sorghum (*S. bicolor* L. *Moench*) is a genus of plants in the grass family, locally known as jawar. Globally grain of sorghum lies fifth in cereals in production. It is widely used as food globally. About half of the production is utilized for human food. It is a chief crop for poor farmers specially in central America, Africa, and South Asia [25].

Alizarin Red S (ARS; anthraquinone dye) belongs to resilient types of dyes that cannot be completely degraded by any biological and physiochemical processes because of its complex aromatic ring structure which is highly stable towards chemical, optical and thermal processes. It has been utilized widely in early times for the dyeing of fibers [26].

Bromophenol Blue (BPB) dye is utilized as a color maker, as a pH indicator, and as a dye. This dye is a derivative of triphenylmethane and related to its close compounds, for example, xanthene and fluorescein that are broadly utilized in drugs, cosmetics, foods, textiles, laboratory indicators, and as printing ink. Many of these related compounds have been stated genotoxic. The structure of dyes are given in Fig. 6.

The basic purpose of this study was to identify the binding sites utilized for the removal of the dye in binding capacity terms. The equilibrium modeling has been used for determination of maximum biosorption capacities and two frequently utilized equilibrium models, that is, Langmuir and Freundlich's models are used for this purpose. Kinetic and thermodynamic modeling has also been employed to study the mechanism and energetics of the process.

2. Materials and methods

Phthalic anhydride ($C_6H_4(CO)_2O$), pyridine (C_5H_5N), and 2-propanol (C_3H_8O) were purchased from Merck (Germany), LABSOLV (India), and Sigma-Aldrich (USA), respectively. All the chemicals were of analytical grade.

Solutions of sodium hydroxide (0.1 mol dm^{-3}) and hydrochloric acid (0.1 mol dm^{-3}) were used for the adjustment of pH. Phthalic anhydride, pyridine, 2-propanol were used for modification of SB. ARS with chemical formula $C_{14}H_7NaO_7S$ (Molecular weight: 342.253 g $mole^{-1}$; λ_{max} = 423 nm) and BPB $C_{19}H_{10}Br_4O_5S$ (Molecular weight: 669.96 g mol^{-1}; λ_{max} = 590 nm) was chosen as substrates for this study.

As an agricultural waste, SB was gathered locally from the Lahore, Pakistan. To remove dirt and water-soluble impurities, it was washed with distilled water. Afterward, the biomass was left for air drying. Dried out SB was grounded and sieved in mesh range of 60–70 ASTM. The specific particle-sized biomass was washed again and again until there is no coloration and dust particle left. It was left for drying at 70°C in the oven and then used for additional investigation and variation. The chemical modification was used by following the methodology of do Carmo Ramos et al. [27,28] with slight modifications.

2.1. Modification of S. bicolor L. with phthalic anhydride

SB (5.0 g) along with phthalic anhydride (8.0 g) was taken in a round bottom flask fitted on a hot plate followed by the addition of pyridine (175 mL). The mixture was magnetically stirred at 300 rpm for 3 h at 100°C. At the end of the reaction, the mixture was allowed to cool in the ice bath for 30 min. Later isopropanol (125 mL) was added in the reaction mixture and again stirred magnetically for 30 min. Afterward, the mixture was filtered to remove the liquor. The modified biosorbent phthalic acid modified *Sorghum* biomass (PASB) was washed sequentially with isopropanol, HCl (0.01 M) and distilled water. The modified biomass was oven-dried at 95°C till constant mass.

2.2. Characterization techniques

The Fourier transform infrared (FTIR) was used to illuminate the main functional groups responsible for binding on the surface of biosorbent. Scanning electron microscopy (SEM) was used to reveal the surface morphology. Furthermore, pH_{pzc} and Boehm's titration was used for the point zero charge valuation and concentration of acidic and basic groups on the surface of biosorbents.

2.3. Biosorption studies

The biosorption process was carried out in batch mode at orbital shaker at 150 rpm to find out the optimal parameters for the adsorption of ARS and BPB like Adsorbent Dosage, Contact Time, Temperature and pH. To obtain optimum

conditions the definite quantity of modified biosorbent (100 mg) was added to dyes solution of known concentration (50 mg L^{-1}, 50 mL for ARS, and 30 mg L^{-1}, 50 mL for BPB) and allowed to stir for a specific time at room temperature in a conical flask (100 mL). After a specific time, the mixture was filtered, and filtrates were analyzed using UV/VISIBLE Research Spectrophotometer (LABOMED, 3500) at specific wavelengths for both dyes. Each parameter is analyzed at every step by keeping constant other factors in the further procedure. The pH effect on sorption mechanism was studied by using NaOH and HCl and to regulate it, pH meter (ADWA-130) was used for this purpose. A kinetic study was achieved at different temperatures to calculate adsorption equilibrium time for each dye. Isotherms modeling were obtained by using different concentrations of dyes. The amount of adsorption (q_{max}) was determined by using the following equations:

$$q_{\max} = \frac{(C_0 - C_e)V}{W} \quad (1)$$

where C_0 is the concentration of the initial dye (mg L^{-1}), C_e is an equilibrium concentration of dyes (mg L^{-1}). V is the volume of solution used (L), and W is the amount of biomass used (g).

The percentage of removal (R%) of dyes can be calculated as:

$$R\% = \frac{(C_0 - C_e)}{C_0} \times 100 \quad (2)$$

3. Results and discussion

3.1. Characterization of PASB

The raw biomass (SB) and modified biomass (PASB) were subjected to FTIR spectrophotometer (Aligent Technologies CARY 630 FTIR). Solid Biomass was placed on an instrument and measures the beam of IR in the form of spectra. The FTIR spectrum of SB is shown in Fig. 1. It indicates the presence of various functional groups which may be the potential binding sites for dye molecules. A broad peak was observed 3,323.30 cm^{-1} indicates the presence of the hydroxyl group (–OH). A peak observed at 2,911.44 cm^{-1} shows the presence of the alkyl group (–R). The spectrum also indicates the presence of the carbonyl (C=O) group at 1,656.08 cm^{-1}. The other fingerprint peaks were observed at 1,395.17; 1,037.83; 738.02 cm^{-1}.

The spectra of PASB are shown in comparison to raw adsorbent in Fig. 1. The broad peak of 3,321.20 cm^{-1} depicts the enhanced hydroxyl group's peaks where mostly binding occurs. The alkyl group shows at 2,917.97 cm^{-1}. The carbonyl group enrichment, that is, 1,726.43 cm^{-1}. The other observed peaks were 1,379.57; 1,252.14; 1,034.57; 902.49; and 656.96 cm^{-1}. The increment in the broadness of peak at 3,321.20 cm^{-1}, shifting of carbonyl peaks and an increase in the intensity of peak at 1,034.57 cm^{-1} affirmed the incorporation of the modifying agent onto the surface of SB.

Raw and modified biosorbents (SB and PASB) were subjected to the SEM (TESCAN Vega LMU, Brno, Czech Republic) and their images obtained are shown in Figs. 2a and b. The SEM images of raw and modified biosorbents reveal their surface morphology. The obtained images show that their surface is highly porous and irregular which facilitates the binding of dyes structure with itself. Comparison of Figs. 2a and b reveal that the modification of raw SB with Phthalic anhydride changes the surface morphology due to its incorporation. This may offer great binding sites of dyes attachment. For this reason, further investigations were carried out on the biosorptive characteristics of PASB.

The point of zero charges is that pH or point where equilibrium is established between negative and positive sites of the adsorbent surface. The charge is neutral at the surface on this point. When a deviation occurs in pH from the point of pH_{pzc} the balance is disturbed [29]. This characterization is very important for the determination of optimal circumstances for the procedure to carry out on a large scale.

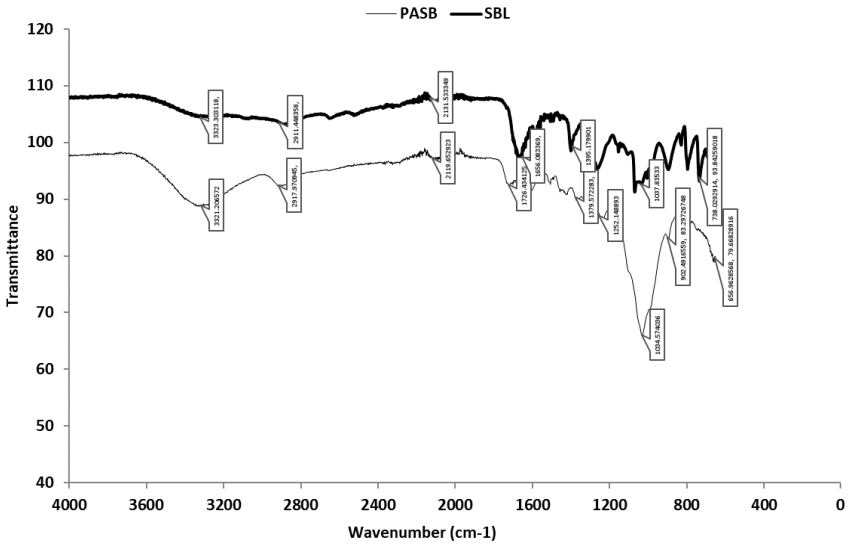

Fig. 1. FTIR spectra of SB and PASB.

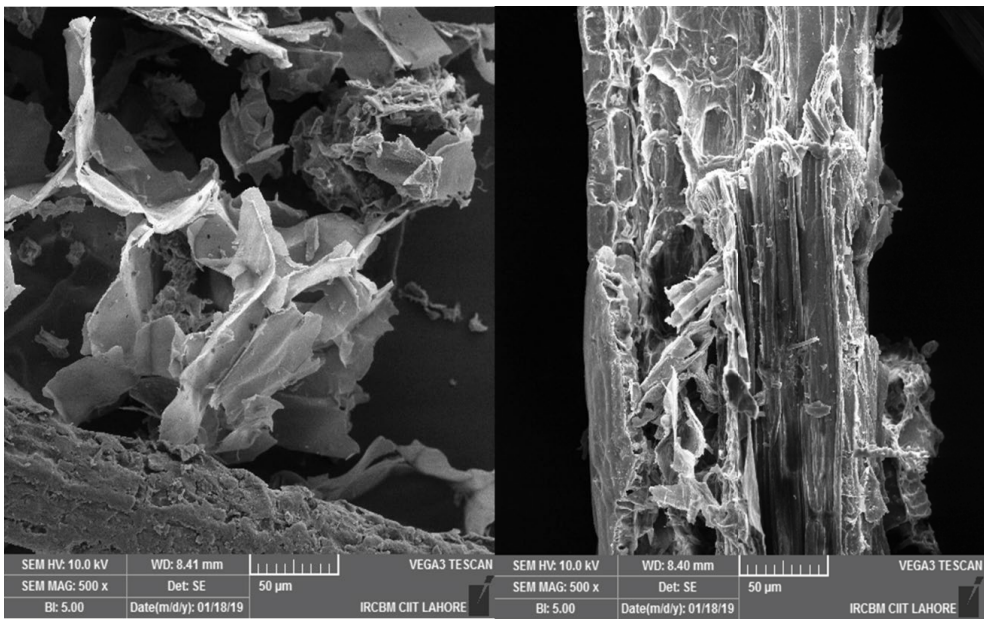

(a) **(b)**

Fig. 2. SEM images of SB (a) and PASB (b) at ×50 μm magnification.

When pH_{pzc} value is greater than the pH than the system was held to be "below the pzc" indicating that the surface is positive due to protonation. While when pH value is greater than pzc than the system was held to be "above the pzc" indicating the net negative charge due to deprotonation.

In Table 1, the value of pHpzc was shown and resulted graph in Fig. 3 shows the cutoff point and gives the value of pHpzc, that is, 3.4 for PASB biomass.

The Boehm's titration was utilized for the determination of acidic and basic groups' concentration. The modified adsorbent interacted with bases and acid (NaOH, Na_2CO_3, $NaHCO_3$, and HCl). By interacting with bases and acid, acidic, and basic functional groups were calculated by utilizing Boehm's titration calculations. The results concentration of acidic and basic groups are shown in Table 1.

Table 1
Characterization of phthalic anhydride modified *Sorghum bicolor L.*

Characterization	Results
pH_{pzc}	3.4
Acidic and basic groups (mmol g–1)	Total acidic groups = 17.5 ± 0.02
	Carboxylic groups = 10.5 ± 0.02
	Lactones = 4.8 ± 0.02
	Phenols = 2.2 ± 0.02
	Total basic groups = 4.5 ± 0.02

3.2. Adsorption of dyes as a function of biosorbent dosage

This factor is important for the determination of equilibrium between sorbent and sorbate for effective removal. The adsorption of BPB and ARS was observed in a batch system. The adsorption process was studied at an initial concentration of 50 and 30 ppm for ARS and BPB respectively. The increasing amount of dosage (0.1–0.9 g) was used in the batch mode at constant initial concentration.

As observed in Fig. 4, it is observed that adsorption capacity is decreasing with an increasing dosage amount. This trend was observed due to the fact that a fixed amount of dyes concentration was used which usually distributes themselves on the surface gradient. It was also observed that the removal percentage increases with an increasing amount of dosage. This may be because of the fact that with an increasing amount of dosage, higher number of active sites are available but after equilibrium was achieved, dye molecules started to accumulate at the surface of adsorbent decreasing the surface area available for molecules and increasing the diffusion path length, so therefore dosage increase doesn't affect the increase in removal percentage. The maximum removal examined was 99.39% and 96.16% for BPB and ARS, respectively.

3.3. Adsorption of dyes as a function of pH

The biosorption as a function of pH was performed in between pH 3 and 10 (adjusted using 0.1 M HCl and 0.1 M NaOH) and variation observed is shown in Fig. 5. For BPB optimum removal was observed at pH around 3 and for ARS around 5–6. This effect was expected as both the dyes are of anionic nature and they prefer acidic pH for attachment with biosorbent surface. The maximum removal observed for BPB at pH 3 was 99.12% with uptake capacity of 14.87 mg g^{-1} and for ARS at pH 6 was 96.15% with uptake capacity of 24.06 mg g^{-1}. Relatively same findings, that is, these dyes prefer acidic medium for optimum attachment, had been observed by previous researchers [30,31]. These results can be described by the molecular structure of the dyes.

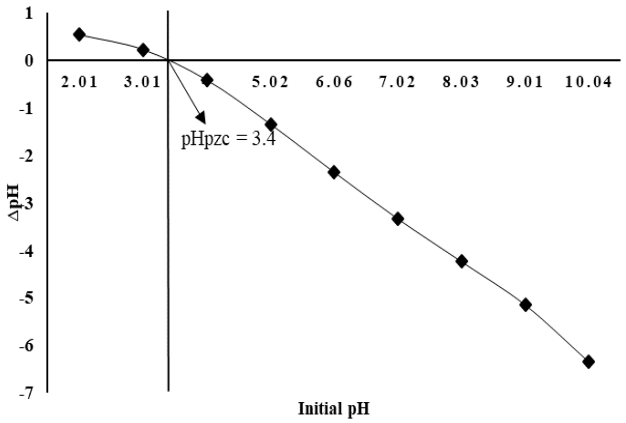

Fig. 3. pH_{pzc} graph for PASB biomass.

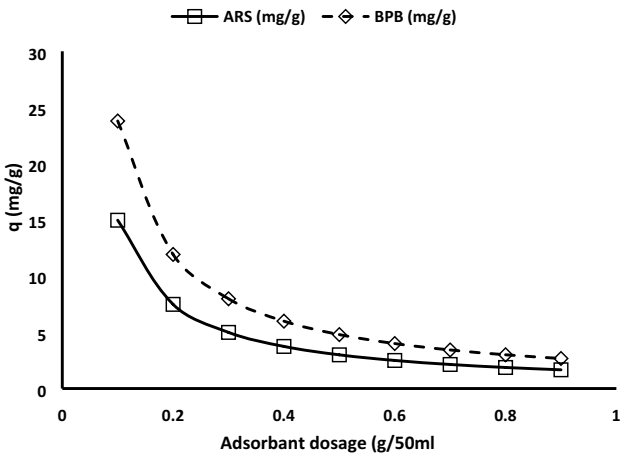

Fig. 4. Effect of PASB dosage on removal of ARS and BPB removal. Initial concentration of ARS: 50 ppm; initial concentration of BPB: 30 ppm; adsorbent dosage: 0.1–0.9 g; time: 25 min.

ARS and BPB belong to the family of anthraquinone and triaryl methane dyes. Their structure is comprised of anions forming colors and has bright colors because of the extended conjugation system of double bonds. When this system interacts with the basic medium with an excess of OH^-, this conjugation system disturbed resulting in the change of color. In acidic medium, the structure of dye is almost unstable and thus disturbance to chromophore change leads to color change.

In the case of ARS, the reddish-orange color of the solution changes to yellow in acidic medium indicating the chromophore change. It almost maintains its structure at pH 5 and above. In the case of BPB, color change occurs below a pH of 4.6.

3.4. Adsorption of dyes as a function of contact time

This process parameter is very significant to get information about the optimum time required for the removal of dyes. It has been reported adsorption process occurs in dual phases [32]. In the initial stage, there is a sharp rise in the adsorption capacity to start due to accessible binding sites at

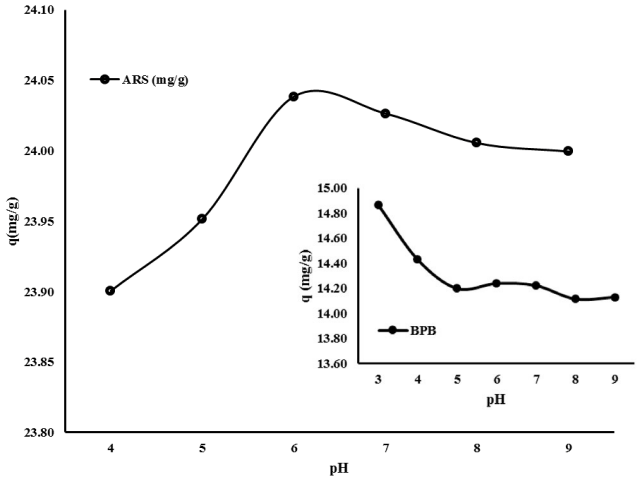

Fig. 5. Effect of pH on the removal of ARS and BPB removal. Initial concentration of ARS: 50 ppm; initial concentration of BPB: 30 ppm; adsorbent dosage: 0.1; time: 25 min.

the surface of biosorbent. In second step capacity decreases because unoccupied sites at the surface were accumulated by dye molecules and thus turn out to be inaccessible. The trend was the same for both dyes. The optimum time was found to be 20–25 min for both dyes. The maximum time of equilibrium achieved at 25 min with a maximum adsorption capacity of 24.06 and 14.89 for ARS and BPB and 24.06 mg g^{-1} correspondingly.

3.5. Kinetic modeling

The optimum time is utilized for the evaluation of the biosorption rate process. It is also used for the determination of sorption mechanism in the system. These representations are used for the determination of biosorption mechanism and determination of rate steps. In addition to information about mechanism, this study is also helpful for the designing of large reactor batch for dyes removal.

The rate equation for pseudo-first-order was developed by Lagergren [33] and its linear form can be represented as:

$$\ln\left(q_e - q_t\right) = \ln q_e - k_1 t \tag{3}$$

where q_e is adsorbed amount of adsorbate (mg g^{-1}), q_t is amount adsorbed at time t (mg g^{-1}), k_1 rate constant (g mg^{-1} min^{-1}), and t is contact time (min). The values of k_1 and q_e for the biosorption of BPB and ARS were evaluated from the linear plot between $\ln(q_e - q_t)$ and t.

Ho and McKay's pseudo-second-order model [34] represent the adsorption capacity and represented in linear form as:

$$\frac{t}{q_t} = \frac{1}{k_2 q_e^2} + \frac{t}{q_e} \tag{4}$$

where q_e is adsorbed amount of adsorbate (mg g^{-1}), q_t is amount adsorbed at time t (mg g^{-1}), k_2 is rate constant (g mg^{-1} min^{-1}), and t is contact time (min). The plot between

t/q_t and t gives a linear relationship. The value of intercept gives $q_{e(\text{cal})}$ and from slope rate constant (k_2) can be calculated.

Percentage difference for adsorption capacity can be calculated as:

$$D\% = \frac{q_{e(\text{cal})} - q_{e(\text{exp})}}{q_{e(\text{exp})}} \times 100 \quad (5)$$

The parameters for the pseudo-first-order kinetics and pseudo-second-order kinetics are given in Table 2 calculated from the plots. The theoretical $q_{e(\text{cal})}$ values for the pseudo-second-order model are closer to the experimental $q_{e(\text{exp})}$ values than those of the pseudo-first-order model. The smaller R^2 and greater D% value for the adsorption of BPB and ARS showed that pseudo-first-order kinetics was not being followed. It was observed from Fig. 7 and the parameters from Table 2 that R^2 value is equal to unity in case of pseudo-second-order rate kinetics and with smaller D% signifying that pseudo-second-order kinetics is being followed by the adsorption process of both dyes.

3.6. Adsorption of dyes as a function of initial dye concentrations

The effect of the initial concentration of dyes on the sorption of BPB and ARS was evaluated at the range of 10–90 mg L^{-1} for both dyes. At minor concentration, all dyes molecules are existing in the solution and interrelate with binding sites easily. However, biosorbent have a restricted number of sites available for binding which turn out to be saturated with the increase in concentration. So, therefore at higher concentrations dye molecules are left behind in the solution which results in the decrease of removal percentage. In contrast, the maximum adsorption capacity for BPB was increased from 4.89 to 43.59 mg g^{-1} and from 4.91 to 43.63 mg g^{-1} for ARS.

3.7. Adsorption isotherms

These isotherms describe how different kinds of adsorbates interact with the adsorbents and that's why are very significant for the mechanism of adsorption for attaining equilibrium and its influence on the surface properties of adsorption. Therefore, adsorption isotherms are necessary for the design of batch mode adsorption [35,36]. These models give us an idea about the relationships between the adsorbent and adsorbate present in the solution at a constant temperature [37]. For the investigation of adsorption isotherm, two models were studied: Langmuir and Freundlich isotherms.

Table 2
Kinetic parameters for the removal of BPB and ARS by PASB

Model	Parameter	BPB	ARS
Pseudo-first-order	k_1 (min^{-1})	0.1305	0.0689
	$q_{e(\text{cal})}$ (mg g^{-1})	2.84	0.0266
	$q_{e(\text{exp})}$ (mg g^{-1})	14.8	24.06
	R^2	0.9712	0.7248
	D%	80.81	99.89
Pseudo-second-order	k_2 (min^{-1})	0.1	8.65
	$q_{e(\text{cal})}$ (mg g^{-1})	15.13	24.06
	$q_{e(\text{exp})}$ (mg g^{-1})	14.8	24.03
	R^2	1	1
	D%	2.23	0.12

The Langmuir model [38] is based on the assumption that monolayer adsorption occurs on the homogenous surface onto a finite number of interaction sites without any interactions. The linear form of the Langmuir model is expressed as:

$$\frac{1}{q_e} = \frac{1}{bq_{\max}} \times \frac{1}{C_e} + \frac{1}{q_{\max}} \quad (6)$$

While its non-linear form is expressed as:

$$q_e = \frac{b \cdot q_m \cdot C_e}{1 + b \cdot C_e} \quad (7)$$

where $q_{\max}$ is the maximum adsorbent capacity (mg g^{-1}), b refers to Langmuir constant, q_e is uptake capacity at equilibrium (mg g^{-1}), and C_e is a concentration of species in solution. The parameters, that is, b and $q_{\max}$ can be determined from the linear plot of $1/q_e$ vs. $1/C_e$ from the slope and intercept.

For the favorable or unfavorable description of adsorption process a separation factor constant R_L which is dimensionless is calculated by the following Eq. (8):

$$R_L = \frac{1}{1 + bC_0} \quad (8)$$

where b is the Langmuir constant and C_0 is initial concentration. This value shows the favorability of isotherm, that is,

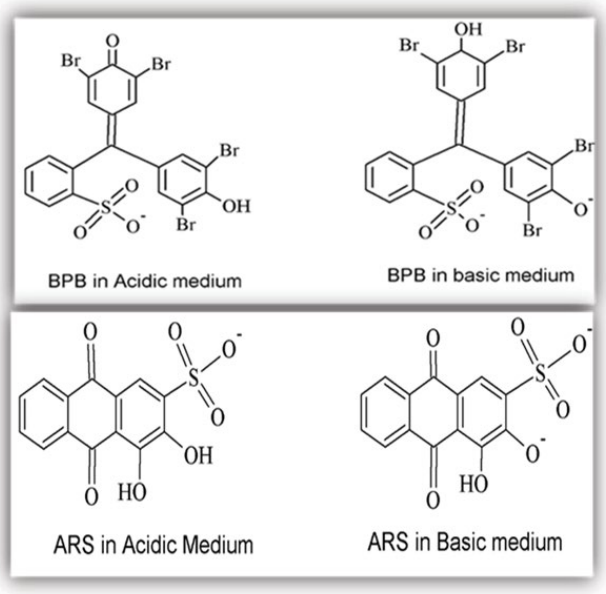

Fig. 6. Structural change of BPB and ARS in acidic and basic medium.

$0 < R_L < 1$, unfavorable ($R_L > 1$), Linear ($R_L = 1$), or irreversible ($R_L = 0$) [39].

It can be seen from correlation coefficients; the experimental data was well explained by the Langmuir model when compared with the Freundlich model for both dyes. This indicates the monolayer coverage of the dyes onto phthalic anhydride modified Sorghum (PASB). The values of R_L show that the Langmuir model is being followed, indicating that adsorptions of BPB and ARS onto PAS were favorable. The Langmuir parameters are given in Table 3 determined from Fig. 8. It was observed that the q_{max} is greater for ARS than that of BPB.

The Freundlich isotherm [40] describes the heterogeneous system of adsorption. It is based on the multilayer adsorption with a nonuniform distribution of adsorbates expressed as:

$$\log q_e = \log K_f + \frac{1}{n}\log C_e \tag{9}$$

While its non-linear form is expressed as:

$$q_e = K_f \times C_e^{1/n} \tag{10}$$

where K_f is Freundlich constant giving adsorption capacity (mg g^{-1}), $1/n$ refers to the intensity of adsorption, q_e is uptake capacity of adsorbent at equilibrium (mg g^{-1}), and C_e is an ionic concentration in solution (mg L^{-1}). The Freundlich constant, n indicates the intensity of adsorption if $1/n < 1$, it shows the favorable adsorption and if $1/n > 1$ than it will be unfavorable system. When n increases adsorption, the bond becomes stronger. Furthermore, $1/n$ is a heterogeneity factor and n shows the deviation measure from linearity. If $n > 1$ than adsorption is favorable by physisorption and if $n < 1$ than adsorption is favored by chemisorption [41]. Linear adsorption is observed when $n = 1$ or near to unity.

It can be seen from the R^2 value that the biosorption of ARS and BPB on PAS biomass did not follow the Freundlich model. As seen from Table 3 higher adsorption intensity was exhibited by BPB than ARS. The value of n was found to be greater in the case of BPB, that is, 1.31 indicating the physisorption than that of ARS having n value less than 1 indicating the chemisorption process.

Table 3
Equilibrium modelling for removal of BPB and ARS by PASB

Model	Parameters	BPB	ARS
	q_{max} (mg g^{-1})	65.78	285.71
	b (L mg^{-1})	0.59	0.043
Langmuir	R_L	0.0184–0.144	0.2045–0.698
	R^2	0.9946	0.9846
	RMSE	0.567347	2.187321
	K_F	21.73	4.65
	n	1.31	0.59
Freundlich	$1/n$	0.763359	1.694915
	R^2	0.9364	0.6322
	RMSE	7.388328	3.012614

The explained models were compared by using the RMSE-the root mean square error values calculated as:

$$\text{RMSE} = \sqrt{\frac{\sum(q_{e(\text{cal})} - q_{e(\text{exp})})^2}{N}} \tag{11}$$

The RMSE value calculated from the non-linear plot was found to be minimum in the case of Langmuir model demonstrating its fitness to our experimental data.

3.8. Adsorption as a function of temperature

The thermodynamics study is used for the feasibility of the adsorption process and its viability for BPB and ARS. The parameters from this study are used for calculating enthalpy ($\Delta H°$), entropy ($\Delta S°$), and free energy ($\Delta G°$). The adsorption capacity of PAS for BPB and ARS increases with increases in temperature as shown in Fig. 9. This trend is maybe because of the opening of new active sites by the increase of temperature. Thermodynamics parameters were calculated by using the following equations and shown in Table 4 [42].

$$\Delta G° = \Delta H° - T\Delta S° \tag{12}$$

$$\Delta G° = -RT\ln K_D \tag{13}$$

$$\ln K_D = \frac{\Delta S°}{R} - \frac{\Delta H°}{RT} \tag{14}$$

where $\Delta G°$ is standard free energy, $\Delta S°$ is the entropy change, $\Delta H°$ is the enthalpy of the process, T contact time (min), R is the universal gas constant (8.314 J mol^{-1} K^{-1}), and K_D is the distribution coefficient calculated as:

$$K_D = \frac{C_0 - C_e}{C_e} \tag{15}$$

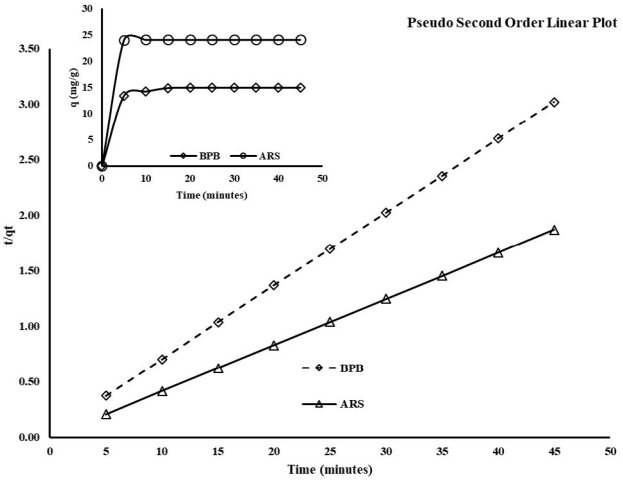

Fig. 7. Effect of contact time on the removal of ARS and BPB removal. Initial concentration of ARS: 50 ppm; initial concentration of BPB: 30 ppm; adsorbent dosage: 0.1; time: 5–45 min.

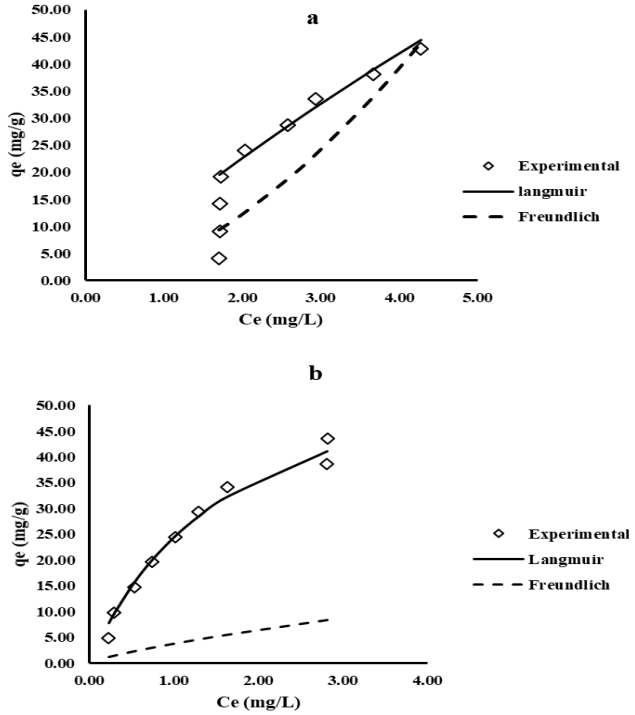

Fig. 8. Non-linear isotherms plot for (a) ARS and (b) BPB depicting the Langmuir and Freundlich models.

The values of $\Delta S°$ and $\Delta H°$ can be determined from intercept and slope from the linear plot of $\Delta G°$ vs. T (K). The values of free energy are calculated by using the value of K at different temperatures. The results are shown in Table 4. The values of $\Delta G°$ are negative in all cases showing a viable and spontaneous process. The negative values of $\Delta H°$ depict that dyes adsorption onto PAS is an exothermic process indicating by the increase of adsorption capacity by an increase in temperature.

As from one deduction magnitude of enthalpy is used for classification of adsorption as physisorption and chemisorption. If bonding strengths are less than 84 kJ mol^{-1} it is considered as physisorption and bond strengths between ranges of 84–420 kJ mol^{-1} referred to chemisorption. Hence, from the value of enthalpy, that is, –5.7045 kJ mol^{-1} for BPB and –7.243 kJ mol^{-1} for ARS indicated the physisorption adsorption. The positive value of $\Delta S°$, that is, 0.0429 for BPB and 0.0296 for ARS showed that dyes adsorption occurs due to the energy redistribution between a small number of molecules which increased by the increase of adsorption which gives a positive value of entropy, hence at solid-surface interaction randomness increases [43].

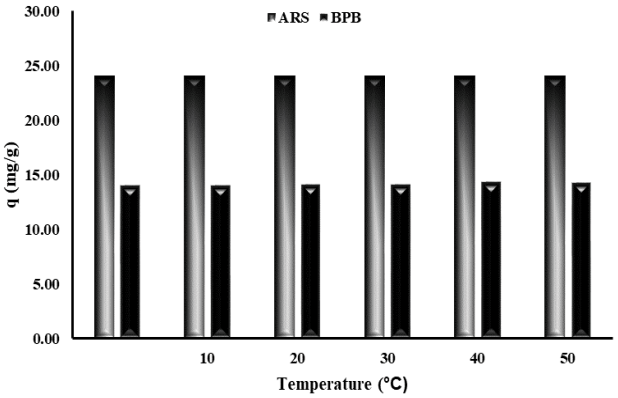

Fig. 9. Effect of temperature on the removal of ARS and BPB by using PASBL. Initial concentration of ARS: 50 ppm; initial concentration of BPB: 30 ppm; adsorbent dosage: 0.1; time: 5–45 min.

3.9. Comparison with other Biosorbents for ARS and BPB removal

Our modifications were also compared with other biosorbents capacities for ARS and BPB removal. The comparison is tabulated in Table 5. The phthalic anhydride modification of *S. bicolor* L. in this study causes the noteworthy variation in the biosorption capacity than the other biosorbent used for the removal of ARS and BPB. Hence, we can say that this modification can be used as potential adsorbent for the ARS and BPB removal from the medium.

Table 4
Thermodynamics parameters for removal of BPB and ARS

Dyes	Temperature (°K)	$\Delta G°$ (kJ mol^{-1})	$\Delta H°$ (kJ mol^{-1})	$\Delta S°$ (kJ mol^{-1})
ARS	283.16	–7.55	–7.24	0.03
	293.16	–7.83		
	303.16	–8.13		
	313.16	–8.43		
	323.16	–8.71		
	333.16	–9.03		
BPB	283.16	–6.24	–5.70	0.04
	293.16	–6.52		
	303.16	–6.90		
	313.16	–7.18		
	323.16	–8.27		
	333.16	–8.13		

Table 5
Comparison of biosorption capacity with other biosorbents

Dyes	Biosorbent used	Adsorptioncapacities ($mg\ g^{-1}$)	References
ARS	PASB	285.71	This study
	Lantana camara	1.165	[31]
	Cynodon dactylon	16.32	[44]
	Magnetic chitosan	40.12	[45]
	Multiwalled carbon nanotubes	161.290	[46]
	Modified nano-sized silica	200	[47]
	Calcined mussel shells	41.75	[48]
	Opuntia ficus indica	118.35	[49]
	Mustard husk	6.08	[50]
BPB	PASB	65.78	This study
	A-chitin nanoparticles	22.72	[51]
	Synthesizing polymer-clay composite	10.78	[52]
	Sorel's cement nanoparticles	4.88	[53]

4. Conclusion

A pioneering phthalic anhydride modified *S. bicolor L.* biosorbent was prepared and its sorption capacity was explored for the removal of reactive dyes, that is, ARS and BPB in a single batch system. Batch studies were conducted, and various parameters were optimized. The optimum dosage was found to be 0.1 g/50 mL for both adsorbates. The optimum time of contact for ARS and BPB was 25 min for both dyes. Optimum pH was found to be 7 or the dye adsorption system works at neutral pH. The maximum adsorption capacities for ARS and BPB were found to be 285.71 and 65.78 mg g^{-1}, respectively. Equilibrium modeling revealed that experimental data fits best in Langmuir's isotherm for both dyes. Parameters like R^2, R_L, and RMSE also support the fitness of Langmuir isotherm. Kinetics modeling shows that data was followed by the pseudo-second-order rate equation indicating the limited rate step mechanism. The parameters of thermodynamics show that the process was exothermic in nature.

References

[1] N. Mohan, N. Balasubramanian, C.A. Basha, Electrochemical oxidation of textile wastewater and its reuse, J. Hazard. Mater., 147 (2007) 644–651.

[2] L. Brinza, C.A. Nygård, M.J. Dring, M. Gavrilescu, L.G. Benning, Cadmium tolerance and adsorption by the marine brown alga *Fucus vesiculosus* from the Irish Sea and the Bothnian Sea, Bioresour. Technol., 100 (2009) 1727–1733.

[3] M.T. Yagub, T.K. Sen, H. Ang, Equilibrium, kinetics, and thermodynamics of methylene blue adsorption by pine tree leaves, Water Air Soil Pollut., 223 (2012) 5267–5282.

[4] Z. Liu, F. Zhang, T. Liu, N. Peng, C. Gai, Removal of azo dye by a highly graphitized and heteroatom doped carbon derived from fish waste: adsorption equilibrium and kinetics, J. Environ. Manage., 182 (2016) 446–454.

[5] F. Deniz, S. Karaman, Removal of an azo-metal complex textile dye from colored aqueous solutions using an agro-residue, Microchem. J., 99 (2011) 296–302.

[6] L. Shi, D. Wei, H.H. Ngo, W. Guo, B. Du, Q. Wei, Application of anaerobic granular sludge for competitive biosorption of methylene blue and Pb(II): fluorescence and response surface methodology, Bioresour. Technol., 194 (2015) 297–304.

[7] M.T. Yagub, T.K. Sen, S. Afroze, H.M. Ang, Dye and its removal from aqueous solution by adsorption: a review, Adv. Colloid Interfaces, 209 (2014) 172–184.

[8] S. Baruah, A. Devi, K. Bhattacharyya, A. Sarma, Developing a biosorbent from *Aegle marmelos* leaves for removal of methylene blue from water, Int. J. Environ. Sci. Technol., 14 (2017) 341–352.

[9] H. Singh, G. Chauhan, A.K. Jain, S. Sharma, Adsorptive potential of agricultural wastes for removal of dyes from aqueous solutions, J. Environ. Chem. Eng., 5 (2017) 122–135.

[10] D. Shen, J. Fan, W. Zhou, B. Gao, Q. Yue, Q. Kang, Adsorption kinetics and isotherm of anionic dyes onto organo-bentonite from single and multisolute systems, J. Hazard. Mater., 172 (2009) 99–107.

[11] J. Song, W. Zou, Y. Bian, F. Su, R. Han, Adsorption characteristics of methylene blue by peanut husk in batch and column modes, Desalination, 265 (2011) 119–125.

[12] S. Wang, H. Li, Dye adsorption on unburned carbon: kinetics and equilibrium, J. Hazard. Mater., 126 (2005) 71–77.

[13] F. Kaouah, S. Boumaza, T. Berrama, M. Trari, Z. Bendjama, Preparation and characterization of activated carbon from wild olive cores (oleaster) by H_3PO_4 for the removal of Basic Red 46, J. Cleaner Prod., 54 (2013) 296–306.

[14] M.M. Sundaram, K.S. Hameed, Adsorption kinetics of crystal violet dye on commercial activated carbon obtained from *Syzygium cumini* seed, J. Chem. Pharm. Res., 4 (2012) 2070–2080.

[15] Z. Aksu, Application of biosorption for the removal of organic pollutants: a review, Process Biochem., 40 (2005) 997–1026.

[16] P. Sharma, B.K. Saikia, M.R. Das, Removal of methyl green dye molecule from aqueous system using reduced graphene oxide as an efficient adsorbent: kinetics, isotherm and thermodynamic parameters, Colloid Surf. A, 457 (2014) 125–133.

[17] M. Doğan, H. Abak, M. Alkan, Adsorption of methylene blue onto hazelnut shell: kinetics, mechanism and activation parameters, J. Hazard. Mater., 164 (2009) 172–181.

[18] U. Etim, S. Umoren, U. Eduok, Coconut coir dust as a low cost adsorbent for the removal of cationic dye from aqueous solution, J. Saudi Chem. Soc., 20 (2016) S67–S76.

[19] X. Han, W. Wang, X. Ma, Adsorption characteristics of methylene blue onto low cost biomass material lotus leaf, Chem. Eng. J., 171 (2011) 1–8.

[20] S. Rangabhashiyam, S. Lata, P. Balasubramanian, Biosorption characteristics of methylene blue and malachite green from

simulated wastewater onto *Carica papaya* wood biosorbent, Surf. Interfaces, 10 (2018) 197–215.
[21] A.H. Jawad, Y. Ngoh, K.A. Radzun, Utilization of watermelon (*Citrullus lanatus*) rinds as a natural low-cost biosorbent for adsorption of methylene blue: kinetic, equilibrium and thermodynamic studies, J. Taibah Univ. Sci., 12 (2018) 1–11.
[22] W. Hassan, U. Farooq, M. Ahmad, M. Athar, M.A. Khan, Potential biosorbent, *Haloxylon recurvum* plant stems, for the removal of methylene blue dye, Arabian J. Chem., 10 (2017) S1512–S1522.
[23] N. Sivarajasekar, R. Baskar, T. Ragu, K. Sarika, N. Preethi, T. Radhika, Biosorption studies on waste cotton seed for cationic dyes sequestration: equilibrium and thermodynamics, Appl. Water Sci., 7 (2017) 1987–1995.
[24] M. Rahimdokht, E. Pajootan, M. Arami, Central composite methodology for methylene blue removal by *Elaeagnus angustifolia* as a novel biosorbent, J. Environ. Chem. Eng., 4 (2016) 1407–1416.
[25] M. Zaroug, I.E. Orhan, F.S. Senol, S. Yagi, Comparative antioxidant activity appraisal of traditional Sudanese kisra prepared from two sorghum cultivars, Food Chem., 156 (2014) 110–116.
[26] S. Pirillo, M.L. Ferreira, E.H. Rueda, The effect of pH in the adsorption of Alizarin and Eriochrome Blue Black R onto iron oxides, 168 (2009) 168–178.
[27] S.N. do Carmo Ramos, A.L.P. Xavier, F.S. Teodoro, M.M.C. Elias, F.J. Goncalves, L.F. Gil, R.P. de Freitas, L.V.A. Gurgel, Modeling mono-and multi-component adsorption of cobalt(II), copper(II), and nickel(II) metal ions from aqueous solution onto a new carboxylated sugarcane bagasse. Part I: batch adsorption study, Ind. Crop Prod., 74 (2015) 357–371.
[28] S.N. do Carmo Ramos, A.L.P. Xavier, F.S. Teodoro, L.F. Gil, L.V.A. Gurgel, Removal of cobalt(II), copper(II), and nickel(II) ions from aqueous solutions using phthalate-functionalized sugarcane bagasse: mono- and multicomponent adsorption in batch mode, Ind. Crop Prod., 79 (2016) 116–130.
[29] D.H.K. Reddy, K. Seshaiah, A. Reddy, S. Lee, Optimization of Cd(II), Cu(II) and Ni(II) biosorption by chemically modified *Moringa oleifera* leaves powder, Carbohydr. Polym., 88 (2012) 1077–1086.
[30] Y. Zeroual, B.S. Kim, C.S. Kim, M. Blaghen, K.M. Lee, Biosorption of bromophenol blue from aqueous solutions by *Rhizopus stolonifer* biomass, Water Air Soil Pollut., 177 (2006) 135–146.
[31] R.K. Gautam, P.K. Gautam, M. Chattopadhyaya, J. Pandey, Adsorption of Alizarin Red S onto biosorbent of *Lantana camara*: kinetic, equilibrium modeling and thermodynamic studies, Proc. Natl. Acad. Sci. India Sect. A, 84 (2014) 495–504.
[32] S.M. Al-Garni, Biosorption of lead by Gram –ve capsulated and non-capsulated bacteria, Water SA, 31 (2005) 345–350.
[33] S. Lagergren, About the theory of so-called adsorption of soluble substances, Sven. Vetenskapsakad. Handingarl, 24 (1898) 1–39.
[34] Y.-S. Ho, G. McKay, Pseudo-second order model for sorption processes, Process Biochem., 34 (1999) 451–465.
[35] B.C.S. Ferreira, F.S. Teodoro, A.B. Mageste, L.F. Gil, R.P. de Freitas, L.V.A. Gurgel, Application of a new carboxylate-functionalized sugarcane bagasse for adsorptive removal of crystal violet from aqueous solution: kinetic, equilibrium and thermodynamic studies, Ind. Crop Prod., 65 (2015) 521–534.
[36] K.Y. Foo, B.H. Hameed, Insights into the modeling of adsorption isotherm systems, Chem. Eng. J., 156 (2010) 2–10.
[37] A. Dubey, S. Shiwani, Adsorption of lead using a new green material obtained from *Portulaca* plant, Int. J. Environ. Sci. Technol., 9 (2012) 15–20.
[38] I. Langmuir, The adsorption of gases on plane surfaces of glass, mica and platinum, J. Am. Chem. Soc., 40 (1918) 1361–1403.
[39] R. Han, H. Li, Y. Li, J. Zhang, H. Xiao, J. Shi, Biosorption of copper and lead ions by waste beer yeast, J. Hazard. Mater., 137 (2006) 1569–1576.
[40] H. Freundlich, About adsorption in solutions, J. Phys. Chem., 57 (1907) 385–470.
[41] A. Murugesan, L. Ravikumar, V. SathyaSelvaBala, P. SenthilKumar, T. Vidhyadevi, S.D. Kirupha, S. Kalaivani, S. Krithiga, S. Sivanesan, Removal of Pb(II), Cu(II) and Cd(II) ions from aqueous solution using polyazomethineamides: equilibrium and kinetic approach, Desalination, 271 (2011) 199–208.
[42] D.H. Everett, The thermodynamics of adsorption. Part II.—Thermodynamics of monolayers on solids, J. Chem. Soc. Faraday Trans., 46 (1950) 942–957.
[43] C.-Y. Kuo, C.-H. Wu, J.-Y. Wu, Adsorption of direct dyes from aqueous solutions by carbon nanotubes: determination of equilibrium, kinetics and thermodynamics parameters, J. Colloid Interface Sci., 327 (2008) 308–315.
[44] J. Samusolomon, P.M. Devaprasath, Removal of Alizarin Red S (Dye) from aqueous media by using *Cynodon dactylon* as an adsorbent, J. Chem. Pharm. Res., 3 (2011) 478–490.
[45] L. Fan, Y. Zhang, X. Li, C. Luo, F. Lu, H. Qiu, Removal of alizarin red from water environment using magnetic chitosan with Alizarin Red as imprinted molecules, Colloids Surf. B, 91 (2012) 250–257.
[46] M. Ghaedi, A. Hassanzadeh, S.N. Kokhdan, Multiwalled carbon nanotubes as adsorbents for the kinetic and equilibrium study of the removal of alizarin red S and morin, J. Chem. Eng. Data, 56 (2011) 2511–2520.
[47] D. Li, Q. Liu, S. Ma, Z. Chang, L. Zhang, Adsorption of Alizarin Red S onto nano-sized Silica modified with γ-aminopropyltriethoxysilane, Adsorpt. Sci. Technol., 29 (2011) 289–300.
[48] M. El Haddad, A. Regti, M.R. Laamari, R. Slimani, R. Mamouni, S. El Antri, S. Lazar, Calcined mussel shells as a new and eco-friendly biosorbent to remove textile dyes from aqueous solutions, J. Taiwan inst. Chem. Eng., 45 (2014) 533–540.
[49] N. Barka, K. Ouzaouit, M. Abdennouri, M. El Makhfouk, Dried prickly pear cactus (*Opuntia ficus* indica) cladodes as a low-cost and eco-friendly biosorbent for dyes removal from aqueous solutions, J. Taiwan inst. Chem. Eng., 44 (2013) 52–60.
[50] R.K. Gautam, A. Mudhoo, M.C. Chattopadhyaya, Kinetic, equilibrium, thermodynamic studies and spectroscopic analysis of Alizarin Red S removal by mustard husk, J. Environ. Chem. Eng., 1 (2013) 1283–1291.
[51] S. Dhananasekaran, R. Palanivel, S. Pappu, Adsorption of methylene blue, bromophenol blue, and coomassie brilliant blue by α-chitin nanoparticles, J. Adv. Res., 7 (2016) 113–124.
[52] A.A. El-Zahhar, N.S. Awwad, E.E. El-Katori, Removal of bromophenol blue dye from industrial waste water by synthesizing polymer-clay composite, J. Mol. Liq., 199 (2014) 454–461.
[53] S. El-Gamal, M. Amin, M. Ahmed, Removal of methyl orange and bromophenol blue dyes from aqueous solution using Sorel's cement nanoparticles, J. Environ. Chem. Eng., 3 (2015) 1702–1712.